GEOLOGY | THE GEOLOGICAL SOCIETY OF AMERICA®

https://doi.org/10.1130/G51497.1

Manuscript received 23 June 2023
Revised manuscript received 25 October 2023
Manuscript accepted 14 November 2023

Published online 29 November 2023

© 2023 The Authors. Gold Open Access: This paper is published under the terms of the CC-BY license.

Marine snowstorm during the Permian–Triassic mass extinction

Stephen E. Grasby[1,*], Omid H. Ardakani[1], Xiaojun Liu[1], David P.G. Bond[2], Paul B. Wignall[3], and Lorna J. Strachan[4]
[1]Geological Survey of Canada, 3303 33rd Street NW Calgary, AB T2L-2A7, Canada
[2]School of Environmental Sciences, University of Hull, Hull HU6 7RX, UK
[3]School of Earth and Environment, University of Leeds, Woodhouse Lane, Leeds LS2 9JT, UK
[4]School of Environment, University of Auckland, Auckland, 1142, New Zealand (Aotearoa)

ABSTRACT

The Permian–Triassic mass extinction (PTME) interval is marked by major excursions in both inorganic and organic carbon (C) isotopes. Carbon cycle models predict that these trends were driven by large increases in productivity, yet organic C–rich rocks are not recorded in most PTME shelf sedimentary successions. Anomalous C-rich facies have been reported from rare abyssal plains records now exposed in Japan and New Zealand, where black shales at the PTME are extraordinarily organic-rich units. We examined organic matter at the Waiheke, New Zealand, section, and results show that these deposits are dominated by lamalginites composed of unicellar solitary or colonial phytoplankton produced during algal blooms that falls as "marine snow." We modeled the impact of ash fall from eruptions in the Siberian Traps large igneous province and argue that they fertilized the Panthalassa Ocean with P and Fe, leading to a marine "snowstorm" and significant C drawdown marking this major biobloom during the PTME.

INTRODUCTION

The Permian–Triassic mass extinction (PTME) was the most severe loss of marine and terrestrial diversity in the Phanerozoic (Bond and Grasby, 2017). Extinction drivers remain debated but are generally considered to have been related to impacts of the Siberian Traps large igneous province (SLIP; Dal Corso et al., 2022). A large negative shift in both organic and inorganic carbon (C) isotope records at the marine extinction level reflects disruption of the global C cycle and contemporaneous changes in productivity. Models suggest that the shift back from this negative C isotope excursion involved increased productivity and C burial (e.g., Schobben et al., 2020; Cui et al., 2021) under anoxic open-ocean conditions (Wignall and Twitchett, 1996). However, enhanced productivity and global C burial are not recorded in shallow shelf and slope successions of latest Permian to earliest Triassic age, which have low organic matter (OM) content, despite extensive anoxia (e.g., Grasby et al., 2019; Müller et al., 2022). The discrepancies between C cycle models and the rock record create a quandary over the interpretation of the C isotope record. The occurrence of "carbonaceous claystone" at the PTME boundary in obducted slices of ocean crust in Japan hints at anomalous organic deposition in the abyssal plains of Panthalassa during the PTME (Isozaki, 1997; Suzuki et al., 1998). Similar deposits from southern Panthalassa are also exposed in New Zealand (Grasby et al., 2021). Here, we show that these deep-sea organic-rich deposits are lamalginites, formed from phytoplankton, which suggest that an open-ocean biobloom occurred during the PTME. As mid-ocean productivity is generally nutrient limited, given the distance from terrestrial input, a transient biobloom is difficult to explain.

Deposition of atmospherically transported volcanic ash is an important source of bioavailable macro- and micronutrients to the mid-ocean. Longman et al. (2021) estimated that 31% of ash-bound P is released from volcanic ash to seawater, and the high Fe content (1–10 wt% FeO) also makes ash a significant source of micronutrients (e.g., Duggen et al., 2010; Xu and Weber, 2021). We modeled the degree of ocean fertilization from SLIP volcanism and show its role as a likely driver of the PTME bioblooms.

Stephen E. Grasby https://orcid.org/0000-0002-3910-4443
*steve.grasby@canada.ca

BACKGROUND

Records of the abyssal plains prior to the Jurassic are extremely rare because of subduction. We examined an outcrop of pelagic sedimentary rocks deposited across the Permian–Triassic boundary (PTB) at the Island Bay section on Waiheke Island, New Zealand (Aotearoa) (Hori et al., 2011; Grasby et al., 2021), located at 36°46.131′S, 175°00.200′E (World Geodetic System 1984 datum). This slice of obducted ocean floor (Fig. 1) records deposition at a paleolatitude of ~34°S (Kodama et al., 2007). Now exposed in an intertidal outcrop, pillow lavas are overlain by organic-lean Upper Permian to Lower Triassic siliceous mudstones and cherts of the Kiripaka Formation (Hori et al., 2011). While paleolongitude is more difficult to ascertain, the absence of terrestrial material and the chert-dominated strata all indicate a deep, open-ocean, abyssal plain sedimentary environment far from continental influence (Hori et al., 2011). These strata host three unique black shale units (units 5, 7, and 9 in Fig. 2; Grasby et al., 2021) that strongly contrast with bounding cherts. The lowest black shale unit (5) is 20 cm thick and spans the PTME. Trace metal and pyrite framboid data from unit 5 suggest that transient euxinic bottom-water conditions developed in the southern Panthalassa Ocean at the PTME, coincident with the globally recognized negative carbon isotope excursion and SLIP eruption (Grasby et al., 2021).

METHODS

Organic matter and its thermal maturity were characterized for 12 newly collected organic-rich samples using reflected light microscopy (Zeiss Axioimager II) equipped with the Diskus-Fossil system. Rock samples were mounted in cold-setting epoxy, which was then polished. The standard reference for reflectance measurement was yttrium-aluminum-garnet, with a 0.906% reflectance under oil immersion.

CITATION: Grasby, S.E., et al., 2024, Marine snowstorm during the Permian–Triassic mass extinction: Geology, v. 52, p. 120–124, https://doi.org/10.1130/G51497.1

Downloaded from http://pubs.geoscienceworld.org/gsa/geology/article-pdf/52/2/120/6199899/g51497.1.pdf
by guest

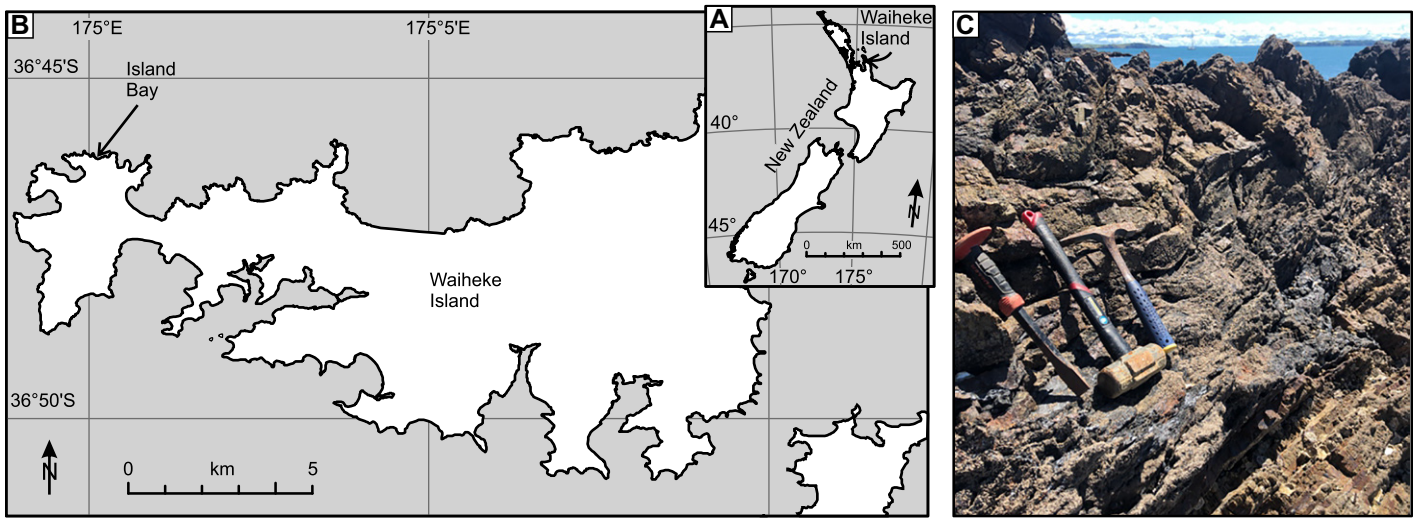

Figure 1. (A, B) Maps showing location of Waiheke section at Island Bay, Waiheke Island, New Zealand, and (C) outcrop photo of black shale unit at Permian–Triassic boundary.

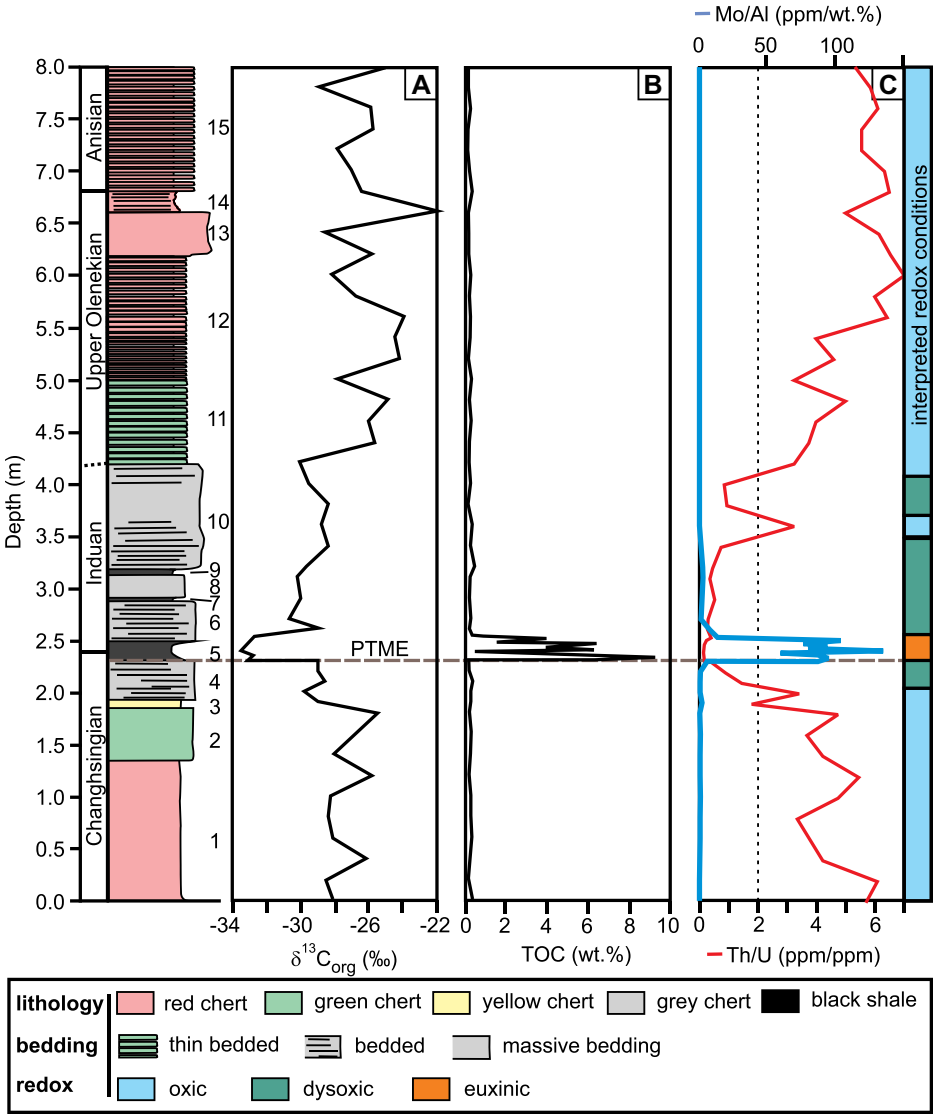

Figure 2. Stratigraphy of Waiheke section, showing (A) carbon isotope record from Grasby et al. (2021), (B) total organic carbon (TOC) content, and (C) proxies for anoxia, Mo/Al and Th/U. $\delta^{13}C$ and elemental proxies are from Grasby et al. (2021). PTME—Permian–Triassic mass extinction.

We modeled P and Fe emissions from the SLIP using a binomial multiplicative cascade, reflecting the fractal nature of LIP eruptions (Grasby et al., 2020). Given uncertainty in eruption length, we modeled SLIP as a series of total potential eruption periods (32, 64, 128, 256, and 512 k.y.). For each eruption period, 100 randomly generated model runs were used to produce a statistical range of results. Ash production was estimated based on Olgun et al. (2011), whereby parameters included: 1:4 ratio of volcaniclastics to lava volume (2.6×10^6 km^3), 5% proportion of ash to volcaniclastics, and a mafic ash density of 2400 kg/m^3. Further details are provided in the Supplemental Material.[1]

RESULTS

Previously reported total organic carbon (TOC) contents of the Waiheke section (Grasby et al., 2021) range from 0.21 to 0.55 wt% (mean = 0.30 wt%), except for the lower black shale (unit 5), where TOC ranges from 0.63 to 9.05 wt % (mean = 4.6 wt%). The thin black shales of units 7 and 9 have TOC values of 0.36 wt% and 0.32 wt%, respectively. Pyrolysis results showed negligible S2 yield, indicating high thermal maturity. Petrographic examination revealed that OM is dominantly marine, bituminized lamalginite that preserves the thin lamellar shape of precursor algae (Fig. 3A). Terrestrially sourced OM (e.g., vitrinite and inertinite) was not observed. Pore-filling pyrobitumen (Fig. 3B) occurs as infill of pore spaces in thin, fine-grained laminae, but it is a minor component of OM, such that TOC dominantly reflects marine algal-matter content. The mean random

[1]Supplemental Material. Additional methods. Please visit https://doi.org/10.1130/GEOL.S.24578989 to access the supplemental material; contact editing@geosociety.org with any questions.

Downloaded from http://pubs.geoscienceworld.org/gsa/geology/article-pdf/52/2/120/6199899/g51497.1.pdf
by guest

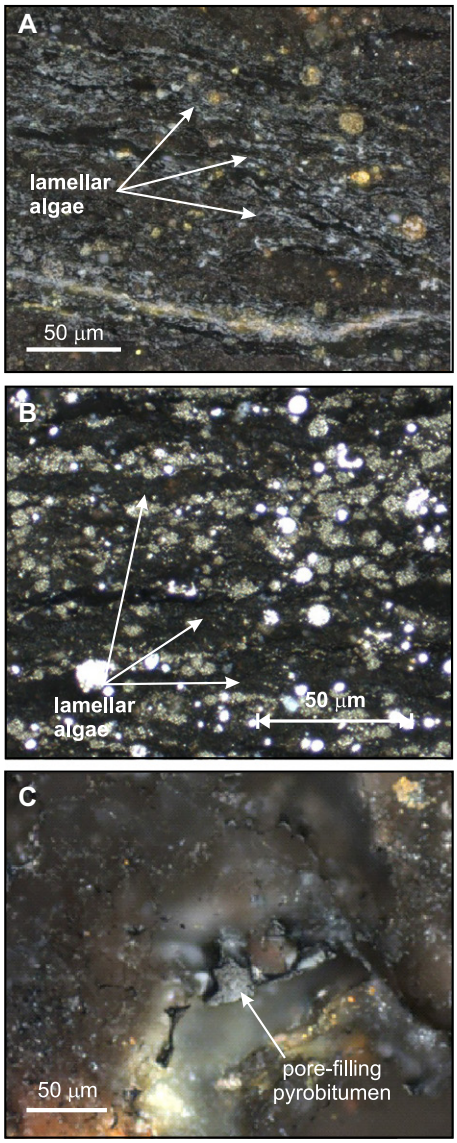

Figure 3. Photomicrographs with incident light under oil immersion, showing: (A) oxidized framboidal pyrites, (A, B) lamellar algae, and (C) minor pore-filling pyrobitumen.

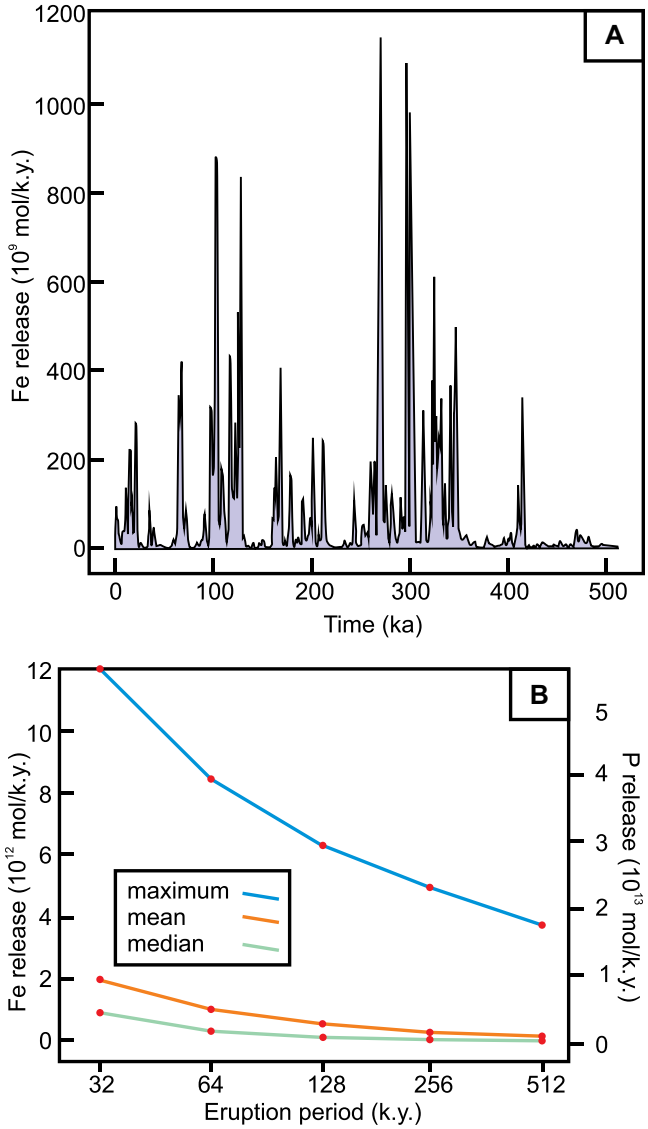

Figure 4. (A) Example plot showing one realization of model for fractal nutrient flux from Siberian Traps eruption. This example is for Fe; a similar pattern would be realized for P. (B) Maximum, mean, and median macronutrient (P) and micronutrient (Fe) flux for 100 eruption model realizations. Patterns for both P and N are similar because they were derived from calculated ash volume; however, absolute loading rates are different.

bitumen reflectance (%BRo) of the lamalginites is 1.2% ± 0.03%, and that of pyrobitumen is 1.8% ± 0.07%. The maximum burial temperature and later thermal alteration events (171 °C and 228 °C, respectively) were estimated using the Barker and Pawlewicz (1994) equation. Using the thermal maturation for the lamalginite, the initial mean and maximum in-place TOC (marine algal content) were determined to be 7.3 wt% and 14.5 wt%, respectively, based on the equation of Jarvie (2012).

Using our model, an example realization (in this case for Fe) for dissolved nutrient loading to the oceans as a function of SLIP eruption rate is shown in Figure 4A. Results from the 100 model runs for each assumed total eruption time gave a range of mean P and Fe fluxes of 5690–91,000 Gmol P/k.y. and 122–1950 Gmol Fe/k.y., respectively (Fig. 4B).

DISCUSSION

Organic-Rich Beds of the Abyssal Plains

At Waiheke, the low TOC content (mean = 0.30 wt%) of sediments other than black shales is consistent with the deep-ocean setting. In contrast to these background conditions, the black shales deposited during the PTME have estimated original mean TOC content of 7.3 wt%, with a maximum of 14.5 wt%, representing extraordinarily high values for abyssal plain sediments.

Organic-rich black shale preservation across the PTME is not unique to this southern Panthalassa site. Black shales reported in sections that represent paleo-equatorial to mid-northern-latitude abyssal plains, now exposed in accretionary complexes of the Chichibu belt and Mino-Tamba terrane of Japan, have been interpreted as evidence for deep-water anoxia at the PTME (Isozaki, 1997). The Japanese records are characterized by deep-water cherts that are replaced in the uppermost Permian section by a siliceous claystone, and then a thin black shale unit that initiates at the PTME and extends into the basal Griesbachian (Isozaki, 1997; Suzuki et al., 1998; Yamakita et al., 1999; Takahashi et al., 2009). The TOC content of the black shales is up to 8 wt% in the Kinkazan area, 3.3 wt% in the Akkamori section (Takahashi et al., 2009), and 7 wt% in the Hisuikyo, Hozukyo, and Kenzan sections, with a mean of 2.56 ± 0.97 wt% (Yamakita et al., 1999). Thus, anomalous organic-rich rocks appear to have been deposited over an extensive area of the Panthalassa abyssal plains during the PTME (from a least mid-southern to mid-northern latitudes). While increased anoxia (Wignall and Twitchett, 1996), which has been shown to have been global by U isotope records (Lau et al., 2016), could explain the preservation of OM, high productivity is required to explain such anomalously high TOC levels in pelagic sediments.

Marine Snowstorm during the Permian–Triassic Mass Extinction

The organic-rich black shales deposited across the PTB at Waiheke are dominated by

Downloaded from http://pubs.geoscienceworld.org/gsa/geology/article-pdf/52/2/120/6199899/g51497.1.pdf
by guest

lamalginite (Fig. 3). Found in Middle Proterozoic to recent sediments (Pickel et al., 2017), lamalginites are composed of unicellular solitary or colonial algae phytoplankton. In marine environments, lamalginite is mainly composed of dinoflagellate and acritarch cysts. Export of this low-density labile OM occurs as "marine snow." Modern marine snow is generally composed of clay as well as organic-derived debris such as the tests of microorganisms, zooplankton fecal pellets, and bacteria (Macquaker et al., 2010). Marine snow accumulation rates are an interplay between rates of biologic production and decomposition of OM en route to the seafloor (e.g., Fowler and Knauer, 1986). Thus, lamalginites typically form during phytoplankton blooms, which enable rapid transport of organic material through the water column.

The thermal maturation of our samples is too high for preservation of biomarkers. However, cholestane/stigmastane ratios in Japanese organic-rich shales indicate a much higher contribution of zoo- and phytoplankton to OM as compared to typical Phanerozoic records (Suzuki et al., 1998), consistent with our observations at Waiheke, where OM is dominated by algal material. Given the distal deep-water setting of the Waiheke section, nutrient levels and productivity would be expected to be very low, in accordance with the organic-lean siliceous sediments bounding the PTME horizon. While anoxia would lead to enhanced OM preservation, as previously interpreted (e.g., Isozaki, 1997), we suggest that the lamalginite deposits at the PTME have their origins in bioblooms. The volume of OM suggests extremely high rates of primary productivity—a veritable marine snowstorm. Such enhanced productivity would require a major nutrient flux to the Panthalassa Ocean, but one that was transient, in order to explain the anomalous organic-rich layers across the PTME in contrast to the OM-lean siliceous sediments deposited before and after the PTME. The estimate of sedimentation rates (0.5 m/m.y.) presented by Hori et al. (2011) constrains the thickest OM-rich bed to record at most 200 k.y. of deposition.

Ocean Fertilization

Primary production in modern oceans is largely confined to narrow shelf regions along western continental margins, and equatorial belts, where upwelling supplies nutrients to the euphotic zone (Boyd et al., 2014). In contrast, oligotrophic subtropical oceans have very low productivity that is almost entirely dependent on near-surface recycling of macronutrients N and P. High-nutrient, low-chlorophyll regions, covering ~40% of world oceans, have productivity limited by the micronutrient Fe (Watson, 2001).

The increased nutrient flux driving a biobloom could come from enhanced continental weathering and runoff, enhanced upwelling of nutrient-rich waters to the photic zone, or enhanced atmospheric loading. The absence of terrestrial OM in our samples along with the distal oceanic setting make direct nutrient loading from increased continental weathering unlikely. Suzuki et al. (1998) argued for increased upwelling in the open ocean during the PTME. However, upwelling is largely restricted to western continental margins (due to Coriolis-driven eastern boundary currents) and equatorial zones (due to Coriolis-driven divergent flow) (e.g., Smith, 1995). While changes in wind shear could have increased equatorial upwelling in some Japanese sections, this is unlikely to account for increased productivity in the midlatitude setting of Waiheke Island. The widespread occurrence of organic-rich sediments across Panthalassa must have involved a broader ocean-wide influence on primary production for up to 200 k.y. Frogner et al. (2001) showed that the instantaneous dissolution of aerosols adsorbed to volcanic ash releases high amounts of P and Fe fast enough to support primary production. Hg concentration spikes and Δ^{199}Hg anomalies at Waiheke Island support the interpretation that enhanced SLIP volcanism was concurrent with lamalginite deposition (Grasby et al., 2021).

Nutrient Loading

The huge scale of basaltic fissure eruptions of the SLIP was capable of injecting ash into the stratosphere (Glaze et al., 2017). Such basaltic ash is more reactive than silicic ash (Jones and Gislason, 2008), ensuring that the SLIP-generated fertilization of the global oceans was likely substantial. In modern time, examples of nutrient release from ash driving bioblooms include the rapid increase (within weeks) of chlorophyll-a in surface waters following the eruptions of Miyake-jima in Japan (Uematsu et al., 2004) and Kasatochi in the Aleutian Islands, United States (Hamme et al., 2010). Volcanic ash has similarly been suggested to have caused major bioblooms in the Late Ordovician (Longman et al., 2021).

Our model results showed a mean range of P and Fe flux of 5690–91,000 Gmol P/k.y. and 122–1950 Gmol Fe/k.y., respectively, and a maximum range of 173,000–559,000 Gmol P/k.y. and 3708–11,970 Gmol Fe/k.y., respectively (dependent on total eruption period of SLIP as in Fig. 4B). In comparison, modern P and Fe dust deposition into the oceans is estimated to be 32,000 and 5700 Gmol/k.y., respectively (Paytan and McLaughlin, 2007; Xu and Weber, 2021). Thus, our results suggest that SLIP nutrient loading would have been in the same order of magnitude as background emissions, at a minimum doubling macro- and micronutrient dust loads to the oceans. Increased P loading is consistent with the globally observed decrease in δ^{15}N values across the PTME (Grasby et al., 2019), as higher P flux would drive enhanced atmospheric N_2 fixation to maintain the 16:1 Redfield N/P ratio. What remains uncertain is why anomalous organic-rich sediments are mainly observed in abyssal plains records across the PTME and not on continental shelves. While anoxic conditions on shelf areas might have been expected to foster organic-rich deposition, the high temperatures experienced in shelf seas may have increased organic remineralization (Wignall, 2015). In a similar sense, preservation bias may be important, where deep-sea records better record a transient biobloom event. The impact of additional nutrient flux on marine productivity would also have been highly variable, controlled by the degree of local deficiency. For instance, Xu and Weber (2021) suggested that the modern Fe supply can range from a strong surplus in areas of upwelling to a strong deficit in subtropical gyres, such that the impact of nutrient loading would be selectively higher in nutrient-deficient open-ocean regions.

CONCLUSIONS

We demonstrated that extraordinarily TOC-rich sediments deposited in deep-ocean settings across the PTME were formed of thick algal deposits, implying the occurrence of major biobloom events creating marine "snowstorms." Our nutrient flux model indicated that the SLIP could have significantly increased P and Fe loading rates to Panthalassa. We suggest that volcanic ash loading can explain the anomalous occurrence of organic-rich deposits in typically nutrient-starved regions of the deep ocean. The surviving ocean-floor records indicate that these layers were extensive and likely constituted a major carbon burial site, as required by models (e.g., Cui et al., 2021) to explain recovery in the δ^{13}C record after the PTME. The organic-poor nature of most contemporary shelf records remains an enigma.

ACKNOWLEDGMENTS

This work benefited from Natural Environment Research Council grant NE/J01799X/1 to D.P.G. Bond.

REFERENCES CITED

Barker, C.E., and Pawlewicz, M.J., 1994, Calculation of vitrinite reflectance from thermal histories and peak temperature: A comparison of methods, *in* Mukhopadhyay, P.K., and Dow, W.G., eds., Vitrinite Reflectance as a Maturity Parameter: American Chemical Society Symposium Series 570, p. 216–229.

Bond, D.P.G., and Grasby, S.E., 2017, On the causes of mass extinctions: Palaeogeography, Palaeoclimatology, Palaeoecology, v. 478, p. 3–29, https://doi.org/10.1016/j.palaeo.2016.11.005.

Boyd, P.W., Sundby, S., and Pörtner, H.-O., 2014, Cross-chapter box on net primary production in the ocean, *in* Field, C.B., et al., eds., Climate Change 2014: Impacts, Adaptation, and Vulnerability. Part A: Global and Sectoral Aspects: Contribution of Working Group II to the Fifth Assessment Report of the Intergovernmental Panel on Climate Change: Cambridge, UK, Cambridge University Press, p. 133–136, https://www.ipcc.ch/report/ar5/wg2/.

Downloaded from http://pubs.geoscienceworld.org/gsa/geology/article-pdf/52/2/120/6199899/g51497.1.pdf
by guest

Cui, Y., Li, M., van Soelen, E.E., Peterse, F., and Kürschner, W.M., 2021, Massive and rapid predominantly volcanic CO_2 emission during the end-Permian mass extinction: Proceedings of the National Academy of Sciences of the United States of America, v. 118, https://doi.org/10.1073/pnas.201470111.

Dal Corso, J., Song, H., Callegaro, S., Chu, D., Sun, Y., Hilton, J., Grasby, S.E., Joachimski, M.M., and Wignall, P.B., 2022, Environmental crises at the Permian–Triassic mass extinction: Nature Reviews–Earth & Environment, v. 3, p. 197–214, https://doi.org/10.1038/s43017-021-00259-4.

Duggen, S., Olgun, N., Croot, P., Hoffmann, L., Dietze, H., Delmelle, P., and Teschner, C., 2010, The role of airborne volcanic ash for the surface ocean biogeochemical iron-cycle: A review: Biogeosciences, v. 7, p. 827–844, https://doi.org/10.5194/bg-7-827-2010.

Fowler, S.W., and Knauer, G.A., 1986, Role of large particles in the transport of elements and organic compounds through the oceanic water column: Progress in Oceanography, v. 16, p. 147–194, https://doi.org/10.1016/0079-6611(86)90032-7.

Frogner, P., Gíslason, S.R., and Óskarsson, N., 2001, Fertilizing potential of volcanic ash in ocean surface water: Geology, v. 29, p. 487–490, https://doi.org/10.1130/0091-7613(2001)029<0487:FPOVAI>2.0.CO;2.

Glaze, L.S., Self, S., Schmidt, A., and Hunter, S.J., 2017, Assessing eruption column height in ancient flood basalt eruptions: Earth and Planetary Science Letters, v. 457, p. 263–270, https://doi.org/10.1016/j.epsl.2014.07.043.

Grasby, S.E., Knies, J., Beauchamp, B., Bond, D.P.G., Wignall, P., and Sun, Y., 2019, Global warming leads to Early Triassic nutrient stress across northern Pangea: Geological Society of America Bulletin, v. 132, p. 943–954, https://doi.org/10.1130/B32036.1.

Grasby, S.E., Liu, X., Yin, R., Ernst, R.E., and Chen, Z., 2020, Toxic mercury pulses into late Permian terrestrial and marine environments: Geology, v. 48, p. 830–833, https://doi.org/10.1130/G47295.1.

Grasby, S.E., Bond, D.P.G., Wignall, P.B., Yin, R., Strachan, L.J., and Takahashi, S., 2021, Transient Permian–Triassic euxinia in the southern Panthalassa deep ocean: Geology, v. 49, p. 889–893, https://doi.org/10.1130/G48928.1.

Hamme, R.C., et al., 2010, Volcanic ash fuels anomalous plankton bloom in subarctic northeast Pacific: Geophysical Research Letters, v. 37, L19604, https://doi.org/10.1029/2010GL044629.

Hori, R.S., et al., 2011, Early Triassic (Induan) Radiolaria and carbon-isotope ratios of a deep-sea sequence from Waiheke Island, North Island, New Zealand: Palaeoworld, v. 20, p. 166–178, https://doi.org/10.1016/j.palwor.2011.02.001.

Isozaki, Y., 1997, Permo-Triassic boundary superanoxia and stratified superocean: Records from lost deep sea: Science, v. 276, p. 235–238, https://doi.org/10.1126/science.276.5310.235.

Jarvie, D.M., 2012, Shale resource systems for oil and gas: Part 1—Shale-gas resource systems, *in* Breyer, J.A., ed., Shale Reservoirs—Giant Resources for the 21st Century: American Association of Petroleum Geologists Memoir 97, p. 69–87.

Jones, M.T., and Gislason, S.R., 2008, Rapid releases of metal salts and nutrients following the deposition of volcanic ash into aqueous environments: Geochimica et Cosmochimica Acta, v. 72, p. 3661–3680, https://doi.org/10.1016/j.gca.2008.05.030.

Kodama, K., Fukuoka, M., Aita, Y., Sakai, T., Hori, R.S., Takemura, A., Campbell, H.J., Hollis, C., Grant-Mackie, J.A., and Spörli, K.B., 2007, Paleomagnetic results from Arrow Rocks in the framework of paleomagnetism in pre-Neogene rocks from New Zealand, *in* Spörli, K.B., et al., eds., The Oceanic Permian/Triassic Boundary Sequence at Arrow Rocks (Oruatemanu), Northland, New Zealand: Lower Hutt, New Zealand, GNS Science Monograph 24, p. 177–196.

Lau, K.V., Maher, K., Altiner, D., Kelley, B.M., Kump, L.R., Lehrmann, D.J., Silva-Tamayo, J.C., Weaver, K.L., Yu, M., and Payne, J.L., 2016, Marine anoxia and delayed Earth system recovery after the end-Permian extinction: Proceedings of the National Academy of Sciences of the United States of America, v. 113, p. 2360–2365, https://doi.org/10.1073/pnas.1515080113.

Longman, J., Mills, B.J.W., Manners, H.R., Gernon, T.M., and Palmer, M.R., 2021, Late Ordovician climate change and extinctions driven by elevated volcanic nutrient supply: Nature Geoscience, v. 14, p. 924–929, https://doi.org/10.1038/s41561-021-00855-5.

Macquaker, J.H.S., Keller, M.A., and Davies, S.J., 2010, Algal blooms and "marine snow": Mechanisms that enhance preservation of organic carbon in ancient fine-grained sediments: Journal of Sedimentary Research, v. 80, p. 934–942, https://doi.org/10.2110/jsr.2010.085.

Müller, J., Sun, Y., Yang, F., Fantasia, A., and Joachimski, M., 2022, Phosphorus cycle and primary productivity changes in the Tethys Ocean during the Permian–Triassic transition: Starving marine ecosystems: Frontiers of Earth Science, v. 10, https://doi.org/10.3389/feart.2022.832308.

Olgun, N., Duggen, S., Croot, P.L., Delmelle, P., Dietze, H., Schacht, U., Óskarsson, N., Siebe, C., Auer, A., and Garbe-Schönberg, D., 2011, Surface ocean iron fertilization: The role of airborne volcanic ash from subduction zone and hot spot volcanoes and related iron fluxes into the Pacific Ocean: Global Biogeochemical Cycles, v. 25, GB4001, https://doi.org/10.1029/2009GB003761.

Paytan, A., and McLaughlin, K., 2007, The oceanic phosphorus cycle: Chemical Reviews, v. 107, p. 563–576, https://doi.org/10.1021/cr0503613.

Pickel, W., et al., 2017, Classification of liptinite—ICCP System 1994: International Journal of Coal Geology, v. 169, p. 40–61, https://doi.org/10.1016/j.coal.2016.11.004.

Schobben, M., et al., 2020, A nutrient control on marine anoxia during the end-Permian mass extinction: Nature Geoscience, v. 13, p. 640–646, https://doi.org/10.1038/s41561-020-0622-1.

Smith, R.L., 1995, The physical processes of coastal ocean upwelling systems, *in* Summerhayes, C.P., et al., eds., Upwelling in the Ocean: Modern Processes and Ancient Records: New York, Wiley, p. 39–64.

Suzuki, N., Ishida, K., Shinomiya, Y., and Ishiga, H., 1998, High productivity in the earliest Triassic ocean: Black shales, southwest Japan: Palaeogeography, Palaeoclimatology, Palaeoecology, v. 141, p. 53–65, https://doi.org/10.1016/S0031-0182(98)00009-1.

Takahashi, S., Yamakita, S., Suzuki, N., Kaiho, K., and Ehiro, M., 2009, High organic carbon content and a decrease in radiolarians at the end of the Permian in a newly discovered continuous pelagic section: A coincidence?: Palaeogeography, Palaeoclimatology, Palaeoecology, v. 271, p. 1–12, https://doi.org/10.1016/j.palaeo.2008.08.016.

Uematsu, M., Toratani, M., Kajino, M., Narita, Y., Senga, Y., and Kimoto, T., 2004, Enhancement of primary productivity in the western North Pacific caused by the eruption of the Miyake-jima Volcano: Geophysical Research Letters, v. 31, L06106, https://doi.org/10.1029/2003GL018790.

Watson, A.J., 2001, Iron limitation in the oceans, *in* Turner, D.R., and Hunter, K.A., eds., The Biogeochemistry of Iron in Seawater: Chichester, UK, John Wiley, p. 9–39.

Wignall, P.B., 2015, The Worst of Times: How Life on Earth Survived Eighty Million Years of Extinction: Princeton, New Jersey, Princeton University Press, 199 p.

Wignall, P.B., and Twitchett, R.J., 1996, Oceanic anoxia and the end Permian mass extinction: Science, v. 272, p. 1155–1158, https://doi.org/10.1126/science.272.5265.1155.

Xu, H., and Weber, T., 2021, Ocean dust deposition rates constrained in a data-assimilation model of the marine aluminum cycle: Global Biogeochemical Cycles, v. 35, https://doi.org/10.1029/2021GB007049.

Yamakita, S., Kadota, N., Kato, T., Tada, R., Ogihara, S., Tajika, E., and Hamada, Y., 1999, Confirmation of the Permian/Triassic boundary in deep-sea sedimentary rocks: Earliest Triassic conodonts from black carbonaceous claystone of the Ubara section in the Tamba belt, Southwest Japan: Journal of the Geological Society of Japan (Chishitsugaku Zasshi), v. 105, p. 895–898, https://doi.org/10.5575/geosoc.105.895.

Printed in the USA

Downloaded from http://pubs.geoscienceworld.org/gsa/geology/article-pdf/52/2/120/6199899/g51497.1.pdf
by guest